journal of the mechanical behavior of biomedical materials 163 (2025) 106898

Contents lists available at ScienceDirect

Journal of the Mechanical Behavior of Biomedical Materials

journal homepage: www.elsevier.com/locate/jmbbm

Regional mechanical properties of spinal cord gray and white matter in transverse section

Nicolas Bailly [a,d,*], Eric Wagnac [b,c,d], Yvan Petit [b,c,d]

[a] LBA UMRT24, Aix Marseille Université/Université Gustave Eiffel, Marseille, France
[b] Ecole de Technologie Supérieure, 1100 Rue Notre Dame O, Montréal, QC, H3C 1K3, Canada
[c] Research Center, CIUSSS Nord de L'île de Montréal, 5400 Boul Gouin O, Montréal, QC, H4J 1C5, Canada
[d] ILab-Spine - Laboratoire International en Imagerie et Biomécanique Du Rachis, France

ARTICLE INFO

Keywords:
Spinal cord
Indentation
Myelin
Microstructure
Soft tissues
Mechanical testing

ABSTRACT

Understanding spinal cord injury requires a comprehensive knowledge of its mechanical properties, which remains debated due to the variability reported. This study aims to characterize the regional mechanical properties of the spinal cord in transverse sections using micro-indentation. Quasi-static indentations were performed on the entire surface of transverse slices obtained from 10 freshly harvested porcine thoracic spinal cords using a 0.5 mm diameter flat punch. No significant difference in average longitudinal elastic modulus was found between white matter ($n = 183$, $E = 0.51 \pm 0.21$ kPa) and gray matter ($n = 51$, $E = 0.53 \pm 0.25$ kPa). In the gray matter, the elastic modulus in the dorsal horn (0.48 ± 0.18 kPa) was significantly smaller than in the ventral horn (0.57 ± 0.24 kPa) (GLMM, $p < 0.05$). The elastic modulus in the dorsal horn was also significantly smaller than in the lateral (0.52 ± 0.22 kPa) and ventral funiculi (0.53 ± 0.18 kPa) of the white matter (GLMM, $p < 0.05$). However, there was no significant difference in the elastic modulus among the ventral, lateral and dorsal funiculi of the white matter (GLMM, $p > 0.05$). The average elastic modulus strongly varies between samples, ranging from 0.23 (± 0.06) kPa to 0.79 (± 0.18) kPa and the testing time postmortem was significantly associated with a decrease in elastic modulus ($t = -5.2$, $p < 0.001$). The spinal cord's white matter demonstrated significantly lower elastic modulus compared to published data on brain tissue tested under similar conditions. These findings enhance our comprehension of the mechanical properties of spinal cord white and gray matter, challenging the homogeneity assumption of current models.

1. Introduction

Every year, worldwide, approximately 900 000 persons suffer from spinal cord injuries or disorder (Ding et al., 2022), which are associated with significant physical, psychological and economic consequences. SCI commonly results from mechanical trauma to the cord, due to road traffic collisions, contact sports, and falls (Chen et al., 2016), but it can also arise from degenerative (e.g. myelopathies) or congenital diseases (e.g. Chiari and syringomyelia) (Noonan et al., 2012). No treatment against SCI neurological consequences has yet been approved although the developments in tissue engineering, regenerative medicine and epidural stimulation are seen as promising solutions (Bartlett et al., 2016; Gorgey et al., 2023). Improving our understanding of injury mechanisms and recovery, as well as advancing treatment effectiveness, requires a deep understanding of the mechanical properties of spinal cord tissues (Bartlett et al., 2016; Fournely et al., 2020; Sparrey et al., 2009). Indeed, spinal cord injuries (SCI) are often caused by mechanical forces (e.g., compression in cervical myelopathy), and these mechanical properties provide insight into how the tissue responds to such forces, which is crucial for understanding damage mechanisms (Lévy et al., 2021). Also, accurate modeling of tissue behavior based on these properties aids in simulating surgical scenarios and predicting outcomes, which is highly beneficial for planning surgical interventions (Wang et al., 2024). Finally, in the fields of tissue-engineering and regenerative medicine, designing biomaterials that mimic the natural mechanical properties of spinal cord tissues is crucial for facilitating effective healing and restoring function (Chen et al., 2024; Jin et al., 2023).

The inner structure of the spinal cord resembles a butterfly and is composed of gray matter, housing neuronal cell bodies, dendrites, and

* Corresponding author. Laboratoire de Biomécanique Appliquée UMR T24 Faculté de médecine, secteur Nord 51, boulevard P. Dramard 13015 Marseille, France.
E-mail address: nicolas.bailly@univ-eiffel.fr (N. Bailly).

https://doi.org/10.1016/j.jmbbm.2025.106898
Received 7 June 2024; Received in revised form 8 January 2025; Accepted 13 January 2025
Available online 13 January 2025

unmyelinated axons. The gray matter is surrounded by white matter, consisting of myelinated axons and an environment that ensures nutrient supply and synaptic remodeling, primarily involving oligodendrocytes, astrocytes and microglia (Budday et al., 2019). Testing white matter and gray matter separately, without influence from the other tissue, is challenging due to the small size of the spinal cord and the complex interweaving of gray matter within the white matter. Nevertheless, researchers have successfully conducted independent tests on both white and gray matters of the spinal cord at different scales. At the cellular level, Koser et al. (2015) used atomic force microscopy (AFM) and showed that gray matter behaves like an isotropic material under compression, while white matter exhibited transversely isotropic behavior, with stiffness strongly correlated to the orientation of axons. At the macroscopic level, various mechanical testing methods have been employed. Sparrey et al. (Sparrey and Keaveny, 2011) and Jannesar et al. (2018) used unconfined compression to characterize the dynamic properties of white matter, demonstrating a highly viscoelastic response. Yu et al. (2020) performed quasistatic confined compression tests on both gray and white matter, finding that both tissues behave as isotropic and viscoelastic materials under compression. Finally, Ozawa et al. (2001) investigated the mechanical stiffness of white and gray matter in various directions using pipette aspiration. Yet, there is no consensus on which of the two materials is stiffer. While Ichihara et al. (2001), Koser et al. (2015) and Yu et al. (2020) suggest that gray matter is stiffer than white matter, Sharkey (2018) reported the opposite. Ozawa et al. (2001) found no significant differences between the two materials.

Studies carried out on the mechanical properties of brain tissue also reported conflicting results on the stiffness of gray and white matter (Budday et al., 2019). According to Budday et al. (2019), this could be partially explained by the difference in the testing conditions reported in the literature. Indeed, gray and white matter were shown to be extremely soft, with a high water content, and to exhibit non-homogeneous, non-linear, viscoelastic behavior, strongly dependent on the type of loading (compression, tension, shear), on the drainage conditions during mechanical tests (confined or not) and on the strain rate (Budday et al., 2019; Zhao et al., 2018; Chatelin et al., 2010). Another explanation for differences in reported gray and white matter stiffness may lie in property variations within white and gray matters. Those variations were recently correlated with the microstructure of the tissues (Budday et al., 2020; Weickenmeier et al., 2016). In a study combining indentation and histological analysis, Weickenmeier et al. (2016) showed that white matter stiffness increased with myelin content and that the white matter of the cerebrum was twice stiffer than the white matter in the cerebellum (Weickenmeier et al., 2016). No studies have been conducted in the spinal cord using similar loading conditions for mechanical testing, making it challenging to draw a direct comparison between the stiffness of white matter in the brain and that in the spinal cord. If significant differences exist between various zones of white matter in the brain, we can hypothesize that similar differences may also occur in the major zones of white matter in the spinal cord. Indeed, spinal cord white matter comprises various ascending and descending tracts, including motor and sensory pathways, which have been well described in human atlases (Lévy et al., 2015). Duval et al. demonstrated that axon morphometries and density vary between these tracts, suggesting that their material properties might also differ (Duval et al., 2019).

This study aims to assess the cross-sectional distribution of mechanical properties within the spinal cord by addressing two key questions: (1) Does gray matter exhibit a higher elastic modulus than white matter in the spinal cord? (2) Is there variability in mechanical properties among the primary zones of the spinal cord (ventral and dorsal horns, anterior, posterior, and lateral funiculi)? To answer these questions, quasi-static micro-indentations were conducted on the surfaces of transverse slices from 10 porcine thoracic spinal cords.

2. Materials and methods

2.1. Mechanical characterization

Ten thoracic spinal cord segments (T2 level) were harvested from 10 porcine spinal cords, prepared within 12 h post-mortem and tested within 17-h post-mortem. To ensure prompt postmortem testing, pigs were obtained from unrelated studies approved by the Institutional Ethics Committee for Animal Research (CIPA) at the CHUM (Centre Hospitalier de l'Université de Montréal). Rather than being discarded, their spinal cords were collected immediately after death to maximize the use of available animal resources. According to the Canadian Council on Animal Care, this procedure required no additional ethics approval. The pigs were Landrace and Yorkshire male pigs, aged between 2 and 3 months, with an average weight of 54 ± 6 kg. The spinal column was extracted within 2 h post-mortem and placed in a refrigerated cooler (approximately 5–10 °C). It was then transported in a to the testing facility in the cooler. A laminectomy was performed to extract spinal cord segments measuring approximately 6 mm in diameter and 5 mm in thickness. They were embedded into agarose at a physiological temperature (gel point at 37 °C) and precise transverse slices were cut using a Compresstome® VF-300-OZ slicing tool, ensuring a smooth and even indentation surface. The thickness of the final samples ranged from 4 to 5 mm. The bottom transverse section of each sample was then glued to a Petri dish to prevent any movement. Samples were submerged in refrigerated phosphate-buffered saline (approximately 5 °C, range 2–12 °C) to minimize deterioration and drying of the tissues and to reduce tissue adhesion with the indenter (Kohn and Ebenstein, 2013; Budday et al., 2017). The phosphate-buffered saline was maintained refrigerated during testing using little PBS ice cubes.

Samples were placed into a Hysitron TI 950 TriboIndenter™ with an XZ 500 extended displacement stage (maximum displacement 500 μm, measurement resolution <0.1 nN, sampling rate 200 Hz). Indentations were performed using a 0.5 mm diameter flat punch. The flat punch has been successfully used to test brain tissues (Weickenmeier et al., 2016, 2017; Budday et al., 2015a) and ensures a constant contact area throughout the indentation process. This simplifies both the detection of initial contact and the calculation of the elastic modulus, as the contact area remains independent of the exact point of initial contact. In order to compare the elastic modulus of the spinal cord and the brain, the testing procedure used on bovine brain by Weickenmeier et al. (2016) was replicated. Indentations were performed with a loading-holding-unloading profile with a maximum displacement of 300 μm, with a loading and unloading rate of 5 μm/s, and a holding time of 10 s (Fig. 1). The indenter's microscope (20x objective lens) was used to identify the boundaries of white and gray matter and to define each indent location. Approximately 18 indents were performed in the white matter and 5 indents in the gray matter per sample. A minimum distance of 0.5 mm was maintained between each indentation and indentations were never performed closer than 0.5 mm from the pia mater. The sequence in which the areas of the cord were indented was defined randomly for each sample. For each indentation, the time was recorded as well as the type of tissue (gray or white matter), the area (ventral or dorsal horn, or anterior, posterior, or lateral funiculi) and the coordinates of the indents in the reference system of the indenter. The overall indentation tests on one sample lasted approximately 3 h.

After the indentation test, methylene blue stain was applied to the samples to delineate the boundary between white and gray matters, after which the samples were photographed. The coordinates of each indent, initially recorded in the reference system of the indenter, were then translated to the reference system of the photograph (see appendix A1). This process ensured that each indentation was accurately labeled according to the correct tissue type (gray or white matter) and region (ventral or dorsal horn, or anterior, posterior, or lateral funiculi). The indents that occurred at the limit between WM and GM (n = 28) were excluded from the statistical analysis.

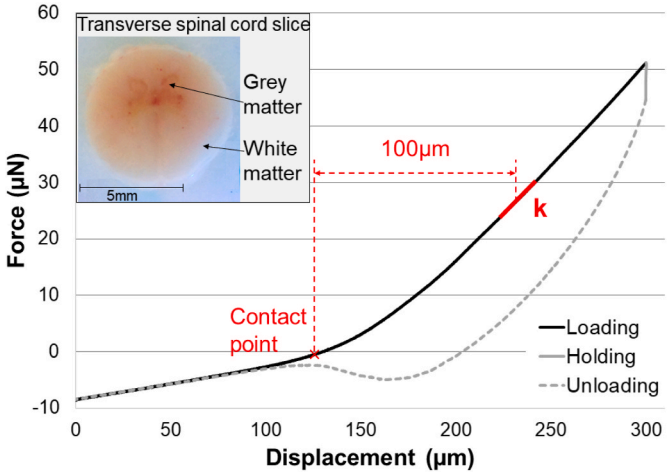

Fig. 1. Transverse spinal cord slice and typical indentation force vs. displacement curves. The contact stiffness k was considered as the slope of the loading curve at a depth of 100 ± 10 µm in the sample (solid red line in the loading curve). (For interpretation of the references to colour in this figure legend, the reader is referred to the Web version of this article.)

2.2. Elastic modulus calculation

Due to the inability of the device to automatically detect the soft tissue surface, the maximum indentation depth varied between each measurement. To ensure that the elastic modulus was consistently measured at the same depth, the contact time between the indenter and the sample was determined retrospectively, and the modulus was calculated from the loading curve, following the approach of Weickenmeier et al. (2016). The contact time between the indenter and the sample was retrospectively identified at the first noticeable change in the slope of the loading curve (Fig. 1). This was done automatically by detecting the changes in the slopes and intercept of the loading curve using the pruned exact linear time method (Killick et al., 2012) implemented using the ischange function in Matlab with a threshold parameter set at 200 (MathWorks, Natick, MA, USA). The contact stiffness k was considered as the slope of the loading curve at a depth of 100 ± 10 µm and was measured by a least-squares linear regression (Fig. 1). The contact stiffness was then used to calculate the effective elastic modulus (Oliver and Pharr, 2004):

$$E_{eff} = \left(\sqrt{\pi}k\right) \Big/ \left(2\sqrt{A}\right) \quad \text{(a)}$$

With $A=1/4\pi d^2$ corresponding to the contact area of the flat punch of diameter d. According to Oliver and Pharr (2004), the relation between the effective elastic modulus E_{eff}, the moduli and poison's ratio of the sample (E_{smp} and ν_{smp}) and indenter (E_{ind} and ν_{ind}) is described by the following:

$$1 \Big/ E_{eff} = \left(1-\nu_{smp}^2\right) \Big/ E_{smp} + \left(1-\nu_{ind}^2\right) \Big/ E_{ind} \quad \text{(b)}$$

Considering that the stiffness of the indenter is orders of magnitude larger than the stiffness of the sample ($E_{ind} \gg E_{smp}$) and that the sample is incompressible $\nu_{smp} = 0.5$ (Budday et al., 2015b), the elastic modulus of the sample is calculated as follows:

$$E_{smp} = \left[1-\nu_{smp}^2\right] E_{eff} = 3k \Big/ 4d \quad \text{(c)}$$

2.3. Statistical analysis

The effects of tissue type (white or gray matter) and post-mortem indentation time on the modulus were evaluated using a Generalized Linear Mixed Model (GLMM), with variability between pig samples treated as a random effect. Normality of the residuals was assessed using the Shapiro-Wilk test (W = 0.99216, p = 0.2767) and homoscedasticity was checked using the testDispersion function from the DHARMa package (dispersion = 1.0364, p-value = 0.824) in R. A similar analysis was performed to study the effect of spinal cord regions (anterior, posterior, and lateral funiculi for WM and ventral and dorsal horn for GM) and of post-mortem indentation time on the elastic modulus.

3. Results

A total of 264 indentations were performed on 10 spinal cord samples. Fig. 2 presents the elastic modulus distribution across these 10 samples. In each sample, variations in elastic modulus were observed between both white and gray matter. However, the location of the peak elastic modulus varied between samples, and no clear pattern could be identified.

Fig. 3(a) compares the elastic modulus measured in the white matter (n = 183) and the gray matter (n = 53) of the 10 spinal cord samples. The mean elastic modulus of all samples was 0.52 (±0.21) kPa for both white matter and for gray matter. No significant difference was found ($p > 0.5$) between the gray and white matter using the Generalized Linear Mixed Model. However, we observed that the time postmortem of the indent significantly decreased the elastic modulus ($t = -5.2$, $p < 0.001$). This is illustrated in Fig. 3(b), which shows a decline in the measured elastic modulus for indentations performed after 12 h postmortem. The average sample elastic modulus also varied between specimens, ranging from 0.23 (±0.06) kPa for sample 7 to 0.79 (±0.18) kPa for sample 10.

Fig. 4 compares the elastic modulus in different regions: ventral and dorsal gray matter horns, and lateral, dorsal, and ventral white matter funiculi. In the gray matter, the elastic modulus in the dorsal horn (0.48 ± 0.18 kPa) was significantly smaller than in the ventral horn (0.57 ± 0.24 kPa) (GLMM, $p < 0.05$). Additionally, the elastic modulus in the dorsal horn was significantly smaller than in the lateral (0.52 ± 0.22 kPa) and ventral funiculi (0.53 ± 0.18 kPa) of the white matter (GLMM, $p < 0.05$). However, no significant difference in the elastic modulus was observed among the three white matter zones (GLMM, $p > 0.05$).

4. Discussion

This study used micro-indentation to investigate the cross-sectional stiffness of the spinal cord. It is a first attempt to map the elastic modulus across the entire transverse section of the spinal cord, offering new experimental indentation data for both gray and white matter at a previously unexplored length scale. Our findings revealed no significant difference in the mean elastic modulus between white matter (WM) and gray matter (GM). However, variations in elastic modulus were observed within both WM and GM regions.

There is currently no consensus in the literature regarding the relative stiffness of white and gray matters. That relative stiffness is important because it impacts the development in tissue engineering as well as the understanding of the strain distribution in the cord during an injury (Fournely et al., 2020). Yu et al. (2020), Ichihara et al. (2001), and Koser et al. (2015) reported that spinal cord gray matter was 1.6–2.1 times stiffer than white matter. In contrast, Ozawa et al. (2001) and the current study found no significant difference in stiffness between the two materials. On the other hand, Sharkey (2018) found in his master's thesis that white matter is stiffer than gray matter. Similarly, contradictory results can be found in the brain, with white matter being sometimes described as stiffer (Budday et al., 2017) and sometime softer (Feng et al., 2013) than gray matter. The magnitude of the equivalent elastic modulus also strongly varied in these studies from 70 Pa (Koser et al., 2015) to more than 200 kPa (Yu et al., 2020). According to Budday et al. (2019), the large variation in white and gray matter mechanical properties could be partially explained by the difference in testing conditions. Indeed, prior studies on spinal cord characterization have exhibited varied loading conditions (Compression in Yu et al. (2020) vs.

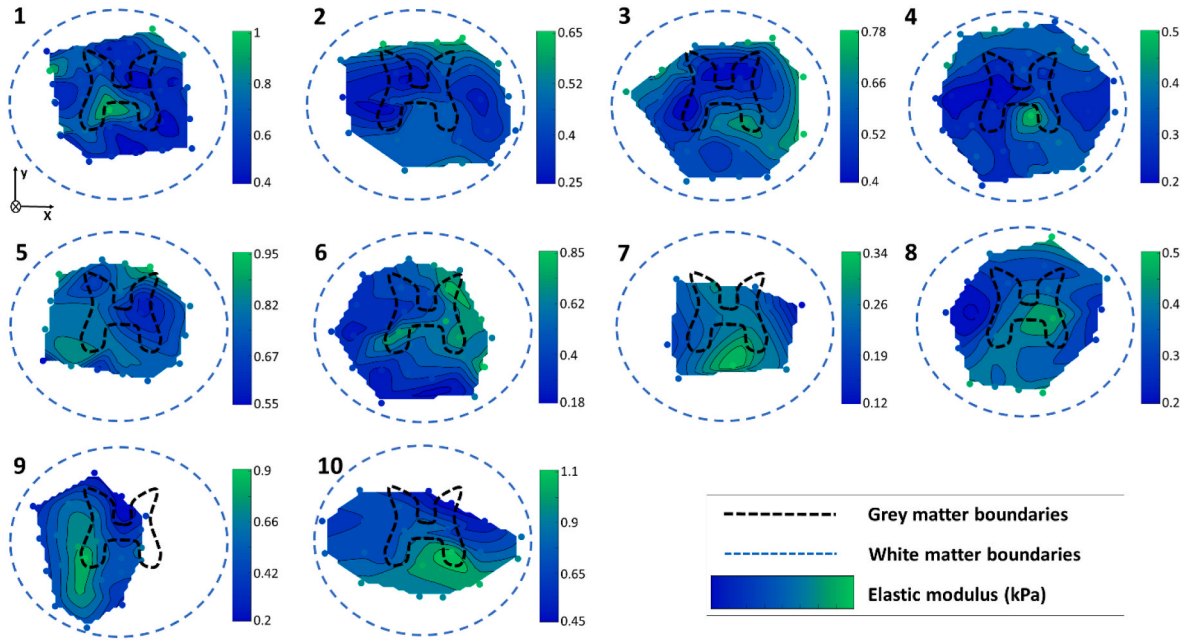

Fig. 2. Elastic modulus distribution across the spinal cord sections of samples 1 to 10. The black and blue dotted lines represent the approximate boundaries of the gray matter and the overall spinal cord, respectively. The surface (contour map) was obtained by fitting the indentation data: the x and y axes represent the indentation coordinates in the schematic spinal cord system, while the z-axis represents the measured modulus. The fitting process involved minimizing the sum of squared errors between the surface and the indentation results, using a piecewise cubic interpolation method. This method was implemented using the fit function in Matlab software (MatWorks, Natick, MA, USA). The method to express the coordinates of each indents from the indentation device into the reference system of a schematic spinal cord is presented in Appendix A. (For interpretation of the references to colour in this figure legend, the reader is referred to the Web version of this article.)

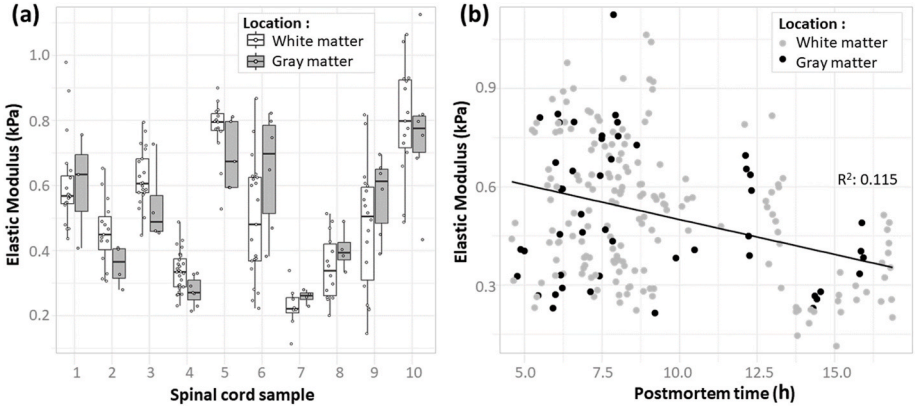

Fig. 3. Elastic modulus of the white and gray matters in the 10-spinal cord (SC) samples (a) and as a function of post-mortem testing time (b). Solid bars, bars, whiskers and dots in (a) represent median values, quartiles, extreme values and individual measurements respectively. The black line in (b) represents a linear regression fit.

tension in Ichihara et al. (2001)), tested scale (from cell-level in Koser et al. (2015) to the entire spinal cord in Ichihara et al. (2001)) and tissue preparation (fresh in Ozawa et al. (2001) vs. flash-frozen in Yu et al. (2020)). Notably, our data showed that the mechanical properties of spinal cord tissues degraded over time postmortem, which may also affect comparisons between studies. This degradation aligns with findings on brain tissue (Mallory et al., 2024), but occurred within 15 h postmortem, faster than the degradation observed for the brain by Budday et al. (2015b) under similar testing conditions.

We chose to perform indentation tests on freshly harvested spinal cord tissue using a 0.5 mm flat punch. This enabled us to test white matter (WM) and gray matter (GM) independently, despite the GM's small butterfly-like shape tangled within the WM. The set-up and methodology were inspired by the work of Budday et al. (2015b), who demonstrated that the method was well suited for testing fresh brain slices. This approach minimizes tissue degradation and dehydration, as well as tissue adhesion, which can have detrimental effects on indentation results (Kohn and Ebenstein, 2013). We found no significant difference between white and gray matter, with a mean elastic modulus of 0.51 ± 0.21 kPa and 0.52 ± 0.25 kPa, respectively. Using a similar setup and loading conditions, Weickenmeier et al., 2016, 2017reported a comparable gray matter elastic moduli in the brain (0.68 ± 0.20 kPa) (Fig. 5). Concerning the white matter, Weickenmeier et al. (2016) found that the white matter in the cerebrum (1.33 ± 0.63 kPa) was as stiff as the white matter of the cerebellum (0.75 ± 0.29 kPa). Our findings suggest that the elastic modulus of the spinal cord's white matter (0.51 ± 0.21 kPa) is even lower than that of the cerebellar white matter. Differences between the two studies may also arise from the animal

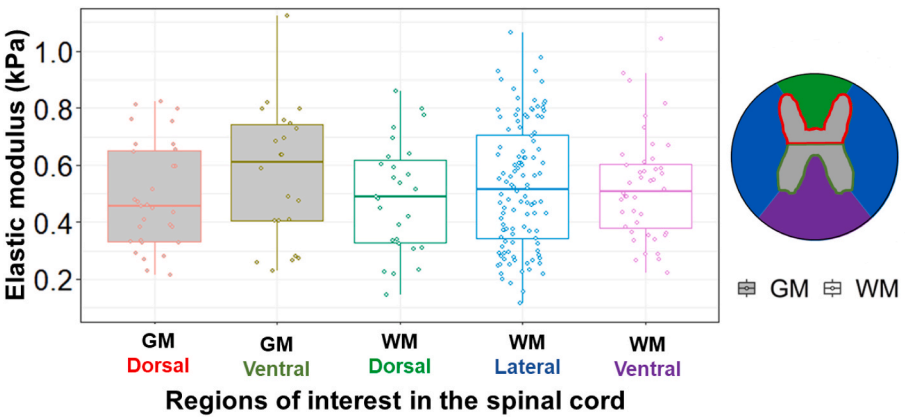

Fig. 4. Elastic modulus measured by indentation in 5 regions of the porcine spinal cord. Solid bars, bars, whiskers and dots represent median values, quartiles, extreme values and individual measurements respectively.

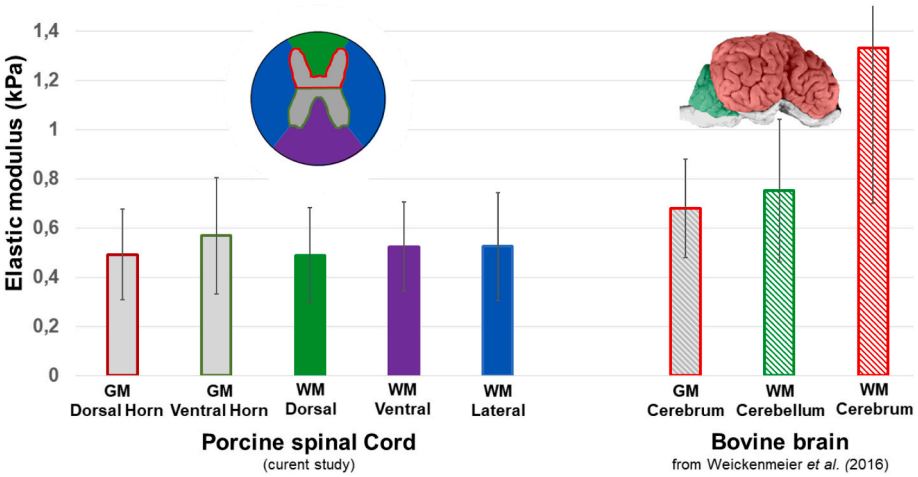

Fig. 5. Mean and standard deviation of elastic modulus of the white matter (WM) and the gray matter (GM) measured by indentation in 5 regions of the porcine spinal cord compared to the bovine brain. The bovine brain results were extracted from (Weickenmeier et al., 2016). The five regions of interest in the spinal cord section: ventral funiculi (n = 44), lateral funiculi (n = 112), dorsal funiculi (n = 27), ventral horn (n = 22) and dorsal horn (n = 31).

model chosen, as we conducted tests on porcine spinal cord, whereas Weickenmeier et al. (2016) used bovine brains. However, according to MacManus et al. (2020), brain tissues' mechanical properties are highly consistent across species. This difference in white matter stiffness suggests that, under quasi-static loading conditions, the mechanical properties of brain white matter should not be used as a substitute for modeling spinal cord white matter.

This study showed some variations of mechanical properties within the gray matter and the white matter (Fig. 5). In the gray matter, we found that the mean standardized elastic modulus was higher in the ventral horn than in the dorsal horn. Interestingly, Koser et al. (2015), using atomic force microscopy in mouse spinal cord, also found that the ventral horn was slightly stiffer than the dorsal horn, but this observation was limited to the transverse section. In the sagittal section, they found the opposite result suggesting that regionally the gray matter is anisotropic and heterogeneous. Koser et al. (2015) proposed that these differences may be due to the preferential craniocaudal orientation of most sensory axons in the dorsal horn, unlike the motor neurons contained in the ventral horn, which did not show a clear directional bias. In the white matter, variations in elastic modulus were expected. Indeed, variations in white matter stiffness have been described between different parts of the brain (e.g., cortex, basal ganglia, corona radiata, and corpus callosum) (Weickenmeier et al., 2016; Budday et al., 2017; Jin et al., 2013; MacManus et al., 2017). Additionally, the structure of the spinal cord's white matter, with tracts of varying axon morphometry and density, suggests that material properties may also vary (Lévy et al., 2015; Duval et al., 2019). However, we did not find any significant differences in the elastic modulus between the ventral, dorsal, and lateral funiculi. While some regions showed higher stiffness within each funiculus, these regions varied between samples, and no clear pattern emerged. This finding is important for future mechanical testing and for advancing current models that consider white and gray matter as either one or two homogeneous materials. Specifically, the difference in stiffness between the ventral and dorsal funiculi in gray matter may influence the stress and strain distribution in the spinal cord under load, and should be considered in mechanical modeling. However, it is important to note that this study is limited to quasi-static stiffness, and local structural differences may affect the viscoelastic behavior of spinal cord. Furthermore, since only one quasi-static condition was tested, this study does not provide sufficient data for the development of a comprehensive constitutive material law for white and gray matters in each region. Nevertheless, the current findings can be used to guide future experimental studies aiming to develop constitutive material laws for spinal cord tissues.

4.1. Limitations

The choice of the indenter as well as the method of modulus calculation was made for both practical and scientific reason but present a few limitations. First, we used a flat punch indenter because its larger,

constant contact area made it easier to define the contact point with the soft spinal cord tissue, allowing us to calculate the modulus without needing precise knowledge of the initial contact point. This also enabled direct comparison with previous brain studies using the same method (Weickenmeier et al., 2016, 2017). However, the edges of the flat punch can cause tissue tearing during deeper indentations (He et al., 2024), necessitating the measurement of the elastic modulus at a relatively shallow depth of 100 μm. Second, since the device was unable to automatically detect the tissue surface, the maximum indentation depth and consequently, the depth of the unloading varied between samples. To ensure that the elastic modulus was consistently measured at the same depth, we retrospectively determined the contact time and calculated the modulus from the loading curve (He et al., 2024). However, the loading portion of the curve reflects a combination of elastic, plastic, and viscoelastic deformations which means that the reported modulus does not represent a purely elastic response. We chose the Oliver and Pharr method for its simplicity, its lower dependency on the accurately defining the contact point, and to enable comparison with prior brain studies that uses the same method (Weickenmeier et al., 2016, 2017). However, while the use of Oliver and Pharr method in the loading phase has been successfully applied to large-strain indentation of soft materials (Delaine-Smith et al., 2016), it is less commonly accepted and used than the Hertzian model in micro- and nano-indentation studies. Finally, the indentation test analysis assumes a continuous, infinite medium, neglecting edge effects and the influence of surrounding tissue supports (He et al., 2024). To minimize these effects, we limited the indentation depth to less than 10% of the sample thickness and ensured that indentations were at least 0.5 mm away from the stiffer pia mater. However, these factors may still influence the measured modulus, meaning that the intrinsic tissue properties may not be fully represented.

The study presents a few other limitations. First, the experiments were performed on porcine spinal cord and the direct translation of those results to human spinal cord has not been demonstrated. MacManus et al. (2020) recently published a study showing that pigs were appropriate surrogates to study human brain mechanical properties but no such work have been performed for spinal cord. Second, all tests were conducted on the thoracic (T2) spinal cord for its central position; however, the results may not fully represent the mechanical properties of WM and GM across all spinal levels. According to Fradet et al. (2016), the cervical, thoracic, and lumbar regions of the spinal cord exhibit different behaviors under transverse compression. Third, the tests were performed ex-vivo, thus neglecting the pretension of the spinal cord which is expected to affect its mechanical properties. To our knowledge, the effect of spinal cord pretension on mechanical properties of the cord has not yet been evaluated. Fourth, our study was limited to the transverse section of the spinal cord and could not inform on the debate whether spinal white and gray matters are isotropic in compression (Koser et al., 2015; Yu et al., 2020). Fifth, due to limited resources, only 10 pigs were included in the study. While this sample size reveals variability in elastic modulus between pigs, it is likely insufficient to fully elucidate the causes of this variability. Sixth, tests were performed up to 15 h post-mortem, and consistent with the literature (Mallory et al., 2024), our data showed that the mechanical properties of spinal cord tissues degraded over time, particularly after 10 h. This may have affected the reported average modulus and comparisons with other studies. Seventh, to minimize tissue deterioration, the samples were tested at a low temperature with the surrounding liquid maintained at approximately 5 °C (with a maximum range of 2 °C–12 °C), which was not precisely controlled throughout the experiment. A recent study has shown that lowering the temperature increases the elastic modulus of spinal cord tissues (Neumann et al., 2024). This may have influenced the measured modulus compared to spinal cord tissue at body temperature and could partly explain variations between samples that were tested at slightly different temperatures. However, we remain confident that the differences observed between the tested areas (i.e., ventral and dorsal horns) are valid, as the testing pattern was randomized to avoid systematic temperature gradients, and temperature differences within a single sample were likely minimal, even if the exact temperatures could not be confirmed. Height, the effect of indenter size was not examined in this study. Budday et al. (2015b) showed that the measured modulus was independent of punch diameter when using flat punches with diameters ranging from 0.75 mm to 1.5 mm on brain tissues. However, the punch diameter used in this study was smaller (0.5 mm), and to the best of our knowledge, no studies have explored this effect on spinal cord tissue. Therefore, it remains possible that the measured modulus may be influenced by indenter size. Ninth, all indentations were performed under the same quasistatic loading condition to identify regional variations and compare them with previous findings in the brain. The material properties obtained at this strain rate are suitable for modeling neurodevelopment, neurodegeneration (Budday et al., 2019), or quasi-static compression, such as in cases of myelopathy (Lévy et al., 2021). However, the viscoelastic properties of the tissue were not assessed, and studies on the brain suggest that the behavior of gray and white matter can vary significantly with increasing loading speeds (MacManus et al., 2018). Consequently, the observed trends between white and gray matter may differ under varying loading rates, and further research is needed to fully understand and model the behavior of spinal cord gray and white matter during traumatic events.

5. Conclusions

Using quasi-static micro-indentation of porcine spinal cord transverse sections, this study suggests that the elastic modulus of WM is not significantly different than that of the GM. Variations in elastic modulus within both WM and GM regions were investigated. In the WM, no significant difference was found between the ventral, dorsal, and lateral funiculi, but in the GM, the ventral horn was found significantly stiffer than the dorsal horn. The stiffness variations measured within the spinal cord GM challenges the current modeling assumption of homogeneous white and gray matter and further work is needed to assess the effect of stiffness variation on spinal cord neurodevelopment as well as on the stress and strain in the cord when loaded. Finally, employing the same indentation method as Weickenmeier et al. (2017) in bovine brain, this study facilitates the comparison between brain and spinal cord findings. It was observed that gray matter stiffness was similar, while the white matter exhibited significantly lower stiffness in the spinal cord. These results supplement the current knowledge on white and gray matter mechanical properties in the spinal cord.

CRediT authorship contribution statement

Nicolas Bailly: Writing – review & editing, Writing – original draft, Methodology, Investigation, Data curation, Conceptualization. **Eric Wagnac:** Writing – review & editing, Supervision, Methodology, Conceptualization. **Yvan Petit:** Writing – review & editing, Supervision, Methodology, Funding acquisition, Conceptualization.

Declaration of AI and AI-assisted technologies in the writing process

During the preparation of this work the author(s) used Deepl and ChatGPT in order to improve readability and language. After using this tool/service, the author(s) reviewed and edited the content as needed and take(s) full responsibility for the content of the publication.

Funding

This work was supported by the Canada Research Chair in Biomechanics of Head and Spine Trauma, file number: 950–231 815.

Declaration of competing interest

The authors declare that they have no known competing financial interests or personal relationships that could have appeared to influence the work reported in this paper.

Appendix A. Supplementary data

Supplementary data to this article can be found online at https://doi.org/10.1016/j.jmbbm.2025.106898.

Data availability

Data will be made available on request.

References

Bartlett, R.D., Choi, D., Phillips, J.B., 2016. Biomechanical properties of the spinal cord: implications for tissue engineering and clinical translation, Regen. Méd. 11, 659–673. https://doi.org/10.2217/rme-2016-0065.

Budday, S., Nay, R., de Rooij, R., Steinmann, P., Wyrobek, T., Ovaert, T.C., Kuhl, E., 2015a. Mechanical properties of gray and white matter brain tissue by indentation. J. Mech. Behav. Biomed. Mater. 46, 318–330. https://doi.org/10.1016/j.jmbbm.2015.02.024.

Budday, S., Nay, R., de Rooij, R., Steinmann, P., Wyrobek, T., Ovaert, T.C., Kuhl, E., 2015b. Mechanical properties of gray and white matter brain tissue by indentation. J. Mech. Behav. Biomed. Mater. 46, 318–330. https://doi.org/10.1016/j.jmbbm.2015.02.024.

Budday, S., Sommer, G., Birkl, C., Langkammer, C., Haybaeck, J., Kohnert, J., Bauer, M., Paulsen, F., Steinmann, P., Kuhl, E., Holzapfel, G.A., 2017. Mechanical characterization of human brain tissue. Acta Biomater. 48, 319–340. https://doi.org/10.1016/j.actbio.2016.10.036.

Budday, S., Ovaert, T.C., Holzapfel, G.A., Steinmann, P., Kuhl, E., 2019. Fifty shades of brain: a review on the mechanical testing and modeling of brain tissue. Arch. Comput. Methods Eng. https://doi.org/10.1007/s11831-019-09352-w.

Budday, S., Sarem, M., Starck, L., Sommer, G., Pfefferle, J., Phunchago, N., Kuhl, E., Paulsen, F., Steinmann, P., Shastri, V.P., Holzapfel, G.A., 2020. Towards microstructure-informed material models for human brain tissue. Acta Biomater. 104, 53–65. https://doi.org/10.1016/j.actbio.2019.12.030.

Chatelin, S., Constantinesco, A., Willinger, R., 2010. Fifty years of brain tissue mechanical testing: from in vitro to in vivo investigations. Biorheology 47, 255–276. https://doi.org/10.3233/BIR-2010-0576.

Chen, Y., He, Y., DeVivo, M.J., 2016. Changing demographics and injury profile of new traumatic spinal cord injuries in the United States, 1972–2014. Arch. Phys. Med. Rehabil. 97, 1610–1619. https://doi.org/10.1016/j.apmr.2016.03.017.

Chen, K., Yu, W., Zheng, G., Xu, Z., Yang, C., Wang, Y., Yue, Z., Yuan, W., Hu, B., Chen, H., 2024. Biomaterial-based regenerative therapeutic strategies for spinal cord injury. NPG Asia Mater. 16, 1–29. https://doi.org/10.1038/s41427-023-00526-4.

Delaine-Smith, R.M., Burney, S., Balkwill, F.R., Knight, M.M., 2016. Experimental validation of a flat punch indentation methodology calibrated against unconfined compression tests for determination of soft tissue biomechanics. J. Mech. Behav. Biomed. Mater. 60, 401–415. https://doi.org/10.1016/j.jmbbm.2016.02.019.

Ding, W., Hu, S., Wang, P., Kang, H., Peng, R., Dong, Y., Li, F., 2022. Spinal cord injury: the global incidence, prevalence, and disability from the global burden of disease study 2019. Spine 47, 1532–1540. https://doi.org/10.1097/BRS.0000000000004417.

Duval, T., Saliani, A., Nami, H., Nanci, A., Stikov, N., Leblond, H., Cohen-Adad, J., 2019. Axons morphometry in the human spinal cord. Neuroimage 185, 119–128. https://doi.org/10.1016/j.neuroimage.2018.10.033.

Feng, Y., Okamoto, R.J., Namani, R., Genin, G.M., Bayly, P.V., 2013. Measurements of mechanical anisotropy in brain tissue and implications for transversely isotropic material models of white matter. J. Mech. Behav. Biomed. Mater. 23, 117–132. https://doi.org/10.1016/j.jmbbm.2013.04.007.

Fournely, M., Petit, Y., Wagnac, E., Evin, M., Arnoux, P.-J., 2020. Effect of experimental, morphological and mechanical factors on the murine spinal cord subjected to transverse contusion: a finite element study. PLoS One 15, e0232975. https://doi.org/10.1371/journal.pone.0232975.

Fradet, L., Cliche, F., Petit, Y., Mac-Thiong, J.-M., Arnoux, P.-J., 2016. Strain rate dependent behavior of the porcine spinal cord under transverse dynamic compression. Proc. Inst. Mech. Eng. [H]. https://doi.org/10.1177/0954411916655373.

Gorgey, A.S., Trainer, R., Sutor, T.W., Goldsmith, J.A., Alazzam, A., Goetz, L.L., Lester, D., Lavis, T.D., 2023. A case study of percutaneous epidural stimulation to enable motor control in two men after spinal cord injury. Nat. Commun. 14, 2064. https://doi.org/10.1038/s41467-023-37845-7.

He, D., Malu, D., Hu, Y., 2024. A comprehensive review of indentation of gels and soft biological materials. Appl. Mech. Rev. 76. https://doi.org/10.1115/1.4065434.

Ichihara, K., Taguchi, T., Shimada, Y., Sakuramoto, I., Kawano, S., Kawai, S., 2001. Gray matter of the bovine cervical spinal cord is mechanically more rigid and fragile than the white matter. J. Neurotrauma 18, 361–367. https://doi.org/10.1089/08977150151071053.

Jannesar, S., Allen, M., Mills, S., Gibbons, A., Bresnahan, J.C., Salegio, E.A., Sparrey, C.J., 2018. Compressive mechanical characterization of non-human primate spinal cord white matter. Acta Biomater. 74, 260–269. https://doi.org/10.1016/j.actbio.2018.05.002.

Jin, X., Zhu, F., Mao, H., Shen, M., Yang, K.H., 2013. A comprehensive experimental study on material properties of human brain tissue. J. Biomech. 46, 2795–2801.

Jin, C., Zhu, R., Wang, Z., Li, Y., Ni, H., Xu, M., Zheng, L., Cao, Y., Yang, Y., Xu, W., Wang, J., Xie, N., Cheng, L., 2023. Dynamic changes in mechanical properties of the adult rat spinal cord after injury. Acta Biomater. 155, 436–448. https://doi.org/10.1016/j.actbio.2022.11.041.

Killick, R., Fearnhead, P., Eckley, I.A., 2012. Optimal detection of changepoints with a linear computational cost. J. Am. Stat. Assoc. 107, 1590–1598. https://doi.org/10.1080/01621459.2012.737745.

Kohn, J.C., Ebenstein, D.M., 2013. Eliminating adhesion errors in nanoindentation of compliant polymers and hydrogels. J. Mech. Behav. Biomed. Mater. 20, 316–326. https://doi.org/10.1016/j.jmbbm.2013.02.002.

Koser, D.E., Moeendarbary, E., Hanne, J., Kuerten, S., Franze, K., 2015. CNS cell distribution and axon orientation determine local spinal cord mechanical properties. Biophys. J. 108, 2137–2147. https://doi.org/10.1016/j.bpj.2015.03.039.

Lévy, S., Benhamou, M., Naaman, C., Rainville, P., Callot, V., Cohen-Adad, J., 2015. White matter atlas of the human spinal cord with estimation of partial volume effect. Neuroimage 119, 262–271. https://doi.org/10.1016/j.neuroimage.2015.06.040.

Lévy, S., Baucher, G., Roche, P.-H., Evin, M., Callot, V., Arnoux, P.-J., 2021. Biomechanical comparison of spinal cord compression types occurring in Degenerative Cervical Myelopathy. Clin. Biomech. 81, 105174. https://doi.org/10.1016/j.clinbiomech.2020.105174.

MacManus, D.B., Pierrat, B., Murphy, J.G., Gilchrist, M.D., 2017. Region and species dependent mechanical properties of adolescent and young adult brain tissue. Sci. Rep. 7, 13729. https://doi.org/10.1038/s41598-017-13727-z.

MacManus, D.B., Murphy, J.G., Gilchrist, M.D., 2018. Mechanical characterisation of brain tissue up to 35% strain at 1, 10, and 100/s using a custom-built micro-indentation apparatus. J. Mech. Behav. Biomed. Mater. 87, 256–266. https://doi.org/10.1016/j.jmbbm.2018.07.025.

MacManus, D.B., Menichetti, A., Depreitere, B., Famaey, N., Vander Sloten, J., Gilchrist, M., 2020. Towards animal surrogates for characterising large strain dynamic mechanical properties of human brain tissue. Brain Multiphysics 1, 100018. https://doi.org/10.1016/j.brain.2020.100018.

Mallory, A., Wetli, A., Neuroth, L.M., Rhule, H., Moorhouse, K., Satterfield, K., Thomas, C., Tesny, A., Kang, Y.-S., 2024. Preservatives for postmortem brain tissue in biomechanical testing: a pilot study. J. Anat. 245, 501–509. https://doi.org/10.1111/joa.14069.

Neumann, O., Surana, H.V., Melly, S., Steinmann, P., Budday, S., 2024. Mechanical characteristics of spinal cord tissue by indentation. J. Mech. Behav. Biomed. Mater. 163, 106863. https://doi.org/10.1016/j.jmbbm.2024.106863.

Noonan, V.K., Fingas, M., Farry, A., Baxter, D., Singh, A., Fehlings, M.G., Dvorak, M.F., 2012. Incidence and prevalence of spinal cord injury in Canada: a national perspective. Neuroepidemiology 38, 219–226. https://doi.org/10.1159/000336014.

Oliver, W.C., Pharr, G.M., 2004. Measurement of hardness and elastic modulus by instrumented indentation: advances in understanding and refinements to methodology. J. Mater. Res. https://doi.org/10.1557/jmr.2004.19.1.3.

Ozawa, H., Matsumoto, T., Ohashi, T., Sato, M., Kokubun, S., 2001. Comparison of spinal cord gray matter and white matter softness: measurement by pipette aspiration method. J. Neurosurg. Spine 95, 221–224. https://doi.org/10.3171/spi.2001.95.2.0221.

Sharkey, L.R., 2018. An Inverse Finite Element Approach to Modeling the Rat Cervical Spinal Cord : for Use in Determining the Mechanical Properties of the Grey and White Matter. University of British Columbia. https://doi.org/10.14288/1.0363918.

Sparrey, C.J., Keaveny, T.M., 2011. Compression behavior of porcine spinal cord white matter. J. Biomech. 44, 1078–1082. https://doi.org/10.1016/j.jbiomech.2011.01.035.

Sparrey, C.J., Manley, G.T., Keaveny, T.M., 2009. Effects of white, grey, and pia mater properties on tissue level stresses and strains in the compressed spinal cord. J. Neurotrauma 26, 585–595. https://doi.org/10.1089/neu.2008.0654.

Wang, H., Zhang, C., Wang, Y., Zeng, Y., Chen, S., Su, X., Li, W., Yu, M., Chen, D., 2024. Biomechanical analysis of spinal cord injury during scoliosis correction surgery. Front. Bioeng. Biotechnol. 12. https://doi.org/10.3389/fbioe.2024.1399691.

Weickenmeier, J., de Rooij, R., Budday, S., Steinmann, P., Ovaert, T.C., Kuhl, E., 2016. Brain stiffness increases with myelin content. Acta Biomater. 42, 265–272. https://doi.org/10.1016/j.actbio.2016.07.040.

Weickenmeier, J., de Rooij, R., Budday, S., Ovaert, T.C., Kuhl, E., 2017. The mechanical importance of myelination in the central nervous system. J. Mech. Behav. Biomed. Mater. 76, 119–124. https://doi.org/10.1016/j.jmbbm.2017.04.017.

Yu, J., Manouchehri, N., Yamamoto, S., Kwon, B.K., Oxland, T.R., 2020. Mechanical properties of spinal cord grey matter and white matter in confined compression. J. Mech. Behav. Biomed. Mater. 112, 104044. https://doi.org/10.1016/j.jmbbm.2020.104044.

Zhao, W., Choate, B., Ji, S., 2018. Material properties of the brain in injury-relevant conditions–Experiments and computational modeling. J. Mech. Behav. Biomed. Mater. 80, 222–234.